The Radio-FIR correlation in the Milky Way

J. Zhang[A], A.Hopkins[A,B], P.J. Barnes[A,C], M. Cagnes[A], Y. Yonekura[D], Y. Fukui[E]

[A] Sydney Institute for Astronomy, School of Physics, University of Sydney, NSW 2006, Australia

[B] Anglo-Australian Observatory, PO Box 296, Epping, NSW 1710, Australia

[C] Astronomy Department, University of Florida, Gainesville, FL 32611, USA

[D] Faculty of Science, Ibaraki University, 2-1-1 Bunkyo, Mito, Ibaraki 310-8512, Japan

[E] Department of Astrophysics, Nagoya University, Furo-cho, Chikusa-ku, Nagoya 464-8602, Japan

Abstract: We investigate the scale on which the correlation between the 843 MHz radio and the 60 μm far-infrared (FIR) emission in the Milky way arises. The correlation is clear on fields of minimum size 30′, corresponding to physical scales of $\approx 20 - 50$ pc. We also investigate the location dependence of $q_{FIR,mean}$, a parameter measuring the radio/FIR ratio. There is a galactic latitude dependence of $q_{FIR,mean}$. If this change in $q_{FIR,mean}$ is interpreted as being dependent on the intensity of star formation activity, the result is consistent with studies of the Large Magellanic Cloud (LMC) and other nearby galaxies.

1 Introduction

The tight correlation between radio and far-infrared (FIR) emission in external galaxies has been long known (e.g. Yun, Reddy & Condon 2001). To explain the correlation, the conventional picture suggests that both emissions are the result of massive star formation. The FIR is mostly thermal emission from dust excited by UV emission associated with star formation. The FIR emission is a common measure of star formation rates (Kennicutt 1998), with associated dust opacity differences in various star forming regions being a concern (Bell 2003). The radio emission has both a thermal component and a non-thermal synchrotron component due to cosmic ray electrons accelerated to relativistic speeds through supernovae shocks.

A complication arises when we note that synchrotron radiation occurs on a larger spatial scale, due to its diffusion length, than the FIR thermal emission. Thus it is expected that the radio-FIR correlation would arise when the observed region around the star formation is large enough to include not only the FIR, but also the emission from the more diffuse cosmic ray electrons. We show that this is indeed true for the Milky Way. Recent studies of the radio-FIR correlation have concentrated on analysing the physical processes which lead to the correlation on galactic scales. This has been done by analysing the correlation on smaller scales (Xu et al. 1992; Hughes et al. 2006). Hughes et al. (2006), looking at the Large Magellanic Cloud (LMC), achieved a spatial resolution of 20 pc. They use the FIR to radio ratio, q_{FIR} as originally defined by Helou, Soifer & Rowan-Robinson (1985). On such fine spatial scales, they were able to demonstrate varying q_{FIR} for different structures in the LMC. In regions of the most active star formation, q_{FIR} is higher. This is interpreted as due to two different physical mechanisms driving the radio-FIR correlation. In the most active star forming regions, radio emission is mostly thermal while in less active regions, the correlation is due to synchrotron radiation. We compute the mean q_{FIR}, called $q_{FIR,mean}$ herein, for images grouped by their galactic latitude. We show that $q_{FIR,mean}$ is elevated closer to the galactic plane, where the most active star formation in our galaxy is occuring, compared to the value in star forming regions at higher galactic latitudes.

2 Analysis

2.1 Data

We investigate the spatial scale on which the radio-FIR correlation begins to arise around star forming regions in the Milky Way. To locate the star forming regions, the Census of High and Medium-mass Protostars (CHaMP) survey conducted with the Mopra dish of the Australia Telescope was used (Barnes et al. 2006). CHaMP targeted 171 dense gas clumps based on the Nanten Survey (Yonekura et al. 2005) of carbon monoxide gas, a useful tracer of the sites of star formation. Using the coordinates from the CHaMP survey, 138 target regions were selected for this analysis based on availability of images. The 843 MHz radio images were obtained from the Sydney University Molonglo Sky Survey (SUMSS; Bock et al. 1999; Mauch et al. 2003) and 60μm (FIR) from the Infrared Astronomical Satellite (IRAS) Sky Survey Atlas (ISSA)[1].

[1]This research has made use of the NASA/ IPAC Infrared Science Archive, which is operated by the Jet Propulsion Laboratory, California Institute of Technology, under contract with the National Aeronautics and Space Administration.

field size (arcmin)	correlation coefficient	$q_{FIR,mean}$	rms scatter
5	0.61	n/a	n/a
10	0.57	n/a	n/a
15	0.64	n/a	n/a
30	0.75	3.19	0.59
60	0.69	3.514	0.50
120	0.81	3.41	0.41

Table 1: The correlation between the FIR and radio emission around regions identified in the CHaMP survey in the Milky Way arises on scales of $30'$ and above. The carbon monoxide tracer used by the CHaMP survey identifies dense gas clumps. Such dense gas clumps could be star forming regions, residuals or pre-stellar gas. This variation could account for a significant portion of the rms scatter.

analysis type	correlation coefficient
initial	0.748
image independence	0.604
major artifacts removed	0.777
FIR noise level subtracted	0.680

Table 2: How the correlation coefficient varies with the refined analysis of 1° images.

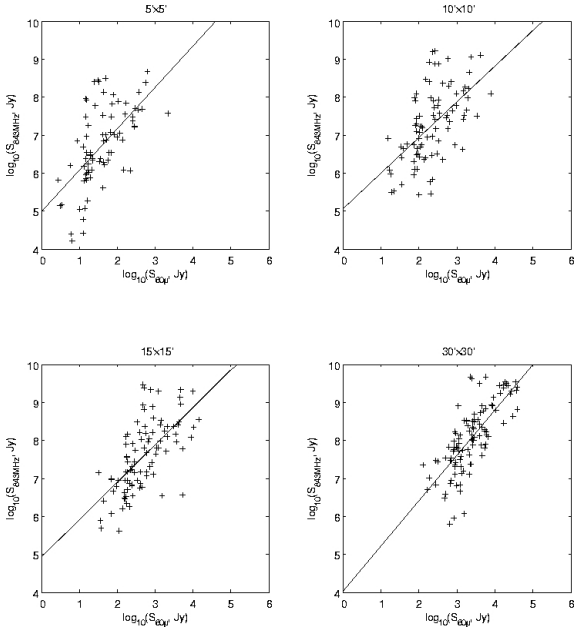

Figure 1: The radio-FIR correlation becomes tight in the $30' \times 30'$ images. This corresponds to a scale of 20 to 50pc

2.2 The Spatial scale on which the correlation arises

For each CHaMP star forming region, SUMSS and ISSA images of varying sizes were obtained. Square field sizes of $5'$, $10'$, $15'$, $30'$, 1° and 2° were analysed. To measure the correlation between the FIR and radio images of the same star forming region, a simple flux sum was taken by adding up the amplitudes of all pixels within the image. The correlation coefficient was calculated for each field size (Table 1). Figure 1 shows radio flux density as a function of FIR flux for the various spatial scales measured.

The images were visually inspected and the analysis refined to ensure the results were not biased by any image artifacts in the radio or noise in the FIR. Artifacts were identified visually and these images excluded. An additional analysis included only images independent by more than 75% of their size. Table 2 shows the variations in the correlation coefficient after accounting for these effects.

Unlike the SUMSS images, the noise in the IRAS images is not centered around zero. The effect of subtracting the mean noise level was analysed using the 1° IRAS images. To subtract the noise level, a histogram of pixel brightnesses allowed identification of the mean background noise.

There was limited data available for the distances to the star forming regions. With the 54 distance measurements out of the 138 identified star forming regions, we can identify the approximate range on which the correlation begins. $30'$ corresponds to a spatial scale of between 22 and 59 pc at distances of 2.5 to 6.8 kpc respectively.

2.3 Analysing q-value variations

The average 60μm FIR to 843 MHz radio ratio of selected images is measured by the $q_{FIR,mean}$ parameter and is defined as follows:

$$q_{FIR,mean} = \langle \log_{10} \left(\frac{S_{60\mu}}{S_{843MHz}} \right) \rangle \qquad (1)$$

Note that this differs from the q_{FIR} typically defined in that here we use different FIR wavelength and radio frequency. This definition of $q_{FIR,mean}$ will not affect the trends observed. The use of 843 MHz rather than 1.4 GHz radio measurements will act to reduce our $q_{FIR,mean}$ by up to 0.15 (for pure synchrotron emission) compared to that of Hughes et al. Using the 60μm flux only, rather than the combined 60μm and 100μm FIR flux reduces our estimate of $q_{FIR,mean}$ by approximately 0.15 again. This systematic offset is slightly smaller than the rms scatter in our measurement (Table 1).

The $q_{FIR,mean}$ is calculated for $30'$, 1° and 2° images where a clear correlation is observed. After correcting the 1° FIR images by subtracting the background noise, $q_{FIR,mean}$ was found to be 3.29. The 1° images were also grouped into two bins to measure any possible galactic latitude dependence of $q_{FIR,mean}$. The

images were divided into two bins containing similar numbers of target regions. For the 1° images, the analysis was repeated for latitudes $|b| \leq 0.8°$ and $|b| > 0.8°$.

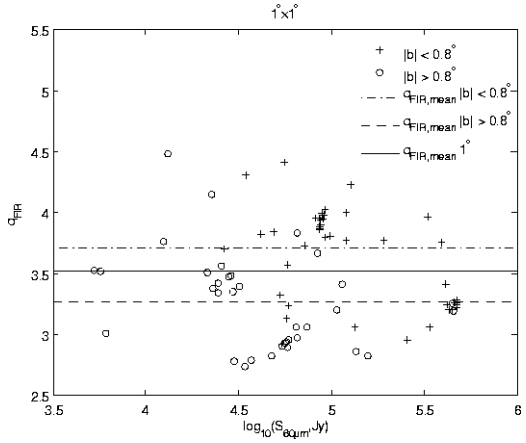

Figure 2: $q_{FIR,mean}$ is elevated closer to the galactic plane, where the star formation is most active. Elevation of q_{FIR} in more active star forming regions has been observed in the LMC (Hughes et al. 2006) and other local galaxies (Murphy et al. 2006).

The $q_{FIR,mean}$ shows a clear galactic latitude dependence, being higher closer to the galactic plane (Figure 2).

3 Discussion

The main results of this investigation are that the local radio-FIR correlation seems to arise on spatial scales of $\approx 20 - 60$ pc and that FIR-radio ratio ($q_{FIR,mean}$) has a galactic latitude dependence. We interpret the second set of results to indicate q_{FIR} is dependent on the level of activity of star formation.

The scale on which the radio-FIR correlation appears around star formation regions is consistent with the LMC study (Hughes et al. 2006) where the correlation arises at ≈ 20 pc and becomes tight above ≈ 50 pc. The diffusion length of relativistic electrons contributing to the galactic FIR-radio ratio ($\approx 1 - 2$ kpc, Bicay & Helou 1990) is much larger than these spatial scales. This suggests that the correlation on such a local scale is between thermal radio and FIR, an interpretation consistent with other studies showing strong correlation between thermal radio and warm dust emission (Hoemes, Berkhuijsen & Xu 1998; Hughes et al. 2006).

The result that q_{FIR} in this study is higher than those on galactic scales is most likely due to missing the synchrotron radio emission that is spread out on larger scales. The result of the latitude dependence analysis strongly suggests there is a dependence of q_{FIR} on the star formation rate. This is based on the assumption that star formation rates are higher closer to the galactic plane. Our results are consistent with those of Hughes et al. (2006), who observed elevated q_{FIR} in the bar of the LMC where there is elevated star formation activity. Strong additional support for our intepretation of the galactic latitude analysis comes from a study of local spiral galaxies. Murphy et al. (2006) observed that active star forming regions of galaxies with lower star formation rate (SFR) display lowered q_{FIR}. Similarly, active star forming regions of galaxies with high SFR displayed elevated q_{FIR}.

From Table 1, the change in $q_{FIR,mean}$ for the three spatial scales is unlikely to be statistically significant given the rms scatter in the measurements. The value of $q_{FIR,mean}$ in the $30'$ images however, is lower than that of both 1° and 2° images by ≈ 0.2. This, while not statistically significant, may imply a suggestive trend. We propose this quick rise in $q_{FIR,mean}$ at $\approx 20-50$ pc and the decrease on larger scales around star forming regions is due to the various components of FIR and radio emission occuring on different spatial scales. The change in $q_{FIR,mean}$ as spatial scale increases is a consequence of the changing proportions of these different components. We can describe the observed behaviour with a simple model for the distribution of these components consistent with the known spatial scales of each emission process.
On the smallest scale, thermal FIR and radio are dominant. The thermal radio emission is due to free-free emission in ionised gas while the thermal FIR emission is from hot dust. On a slightly larger scale, cirrus FIR emission continues to contribute, eventually ceasing and leaving only the synchrotron radiation component on the largest scale.
A simple model demonstrates that the rise in $q_{FIR,mean}$ between the $30'$ and the 1° images could be due to the thermal radio emission falling off faster around star forming regions than the thermal FIR emission. On the kiloparsec scale, q_{FIR} would decrease with the increasing contribution of the synchrotron radiation while the FIR emission has ceased. This simple model is illustrated in Figure 3.

4 Conclusion

We have examined the scale on which the radio-FIR correlation arises around star forming regions of the Milky Way. The correlation appears on scales of $\approx$ 20–60 pc. The galactic latitude dependence of $q_{FIR,mean}$ is consistent with that found in the LMC and local spiral galaxies (Hughes et al, 2006 and Murphy et al, 2006), and strongly suggests that q_{FIR} is elevated in more active star forming regions.
We have suggested a simple model that accounts for these observed trends in $q_{FIR,mean}$. To test this model, we plan to compare individual q_{FIR} values with the di-

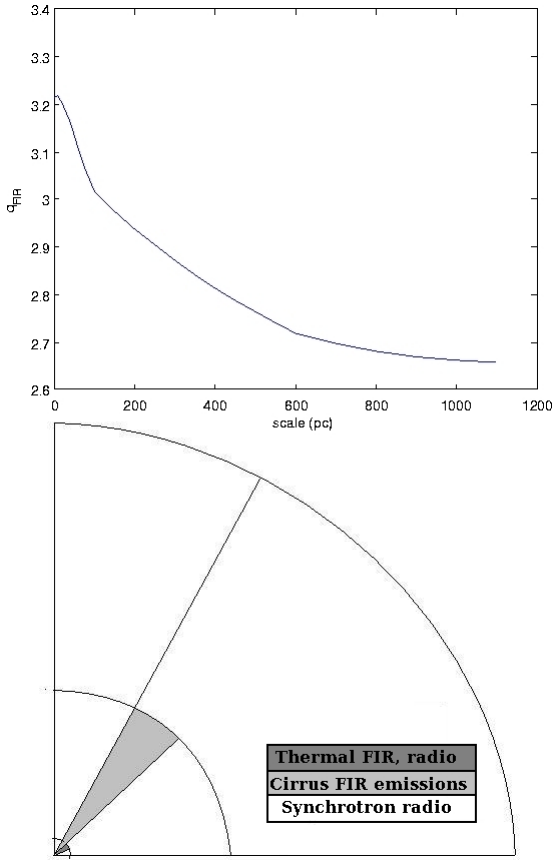

Figure 3: A simple model of the scale on which the components of FIR and radio emission extend beyond the star forming region.

rectly measured star formation rates in each CHaMP target region.
Multifrequency radio continuum measurements around each could allow determination of the thermal-to-synchrotron ratio as a function of spatial scale. This would provide a more accurate quantitative constraint on the scales within the simple model proposed here.

5 References

Barnes P.J. et al., 2006, in IAU Symposium 231: Astrochemistry Throughout the Universe, D. Lis, G.A. Blake, E. Herbst (eds.) (Cambridge UP: Cambridge)

Bell E., 2003, ApJ, 586, 794

Bicay M.D., & Helou G., 1990, ApJ, 362, 59

Bock D., Large M.I., Sadler E.M., 1999, AJ, 117, 1578

Helou G., Soifer B.T., Rowan-Robinson M., 1985, ApJ, 298, L7

Hoemes P., Berkhuijsen E.M., Xu C., 1998

Hughes A., Wong T., Ekers R., Staveley-Smith L., Filipovic M., Maddison S., Fukui Y., Mizuno N., 2006, Mon. Not. R. Astron. Soc. 370, 363-379

Kennicutt R.C. Jr, 1998, ARAA, 36, 189K

Mauch T., Murphy T., Buttery H.J., Curran J., Hunstead R.W., Piestrzynska B., Robertson J.G., Sadler E.M., 2003, MNRAS, 342, 1117

Murphy E.J. et al., 2006, ApJ, 651L, 111

Yonekura et al., 2005, ApJ, 634, 476

Yun M.S., Reddy N.A., and Condon J.J., 2001, ApJ, 554, 803